Effects of non-thermal mobile phone radiation on breast adenocarcinoma cells

Authors:
Barend A. Stander[1]
Sumari Marais[1]
Carin Huyser[2]
Zen Fourie[3]
Dariusz Leszczynski[4]
Annie M. Joubert[1]

Affiliations:
[1]Department of Physiology, University of Pretoria, Pretoria, South Africa

[2]Reproductive Biology Laboratory, Department of Obstetrics and Gynaecology, University of Pretoria, Pretoria, South Africa

[3]South African Bureau of Standards, Pretoria, South Africa

[4]Functional Proteomics Group, Radiation Biology Laboratory, STUK Radiation and Safety Authority, Helsinki, Finland

Correspondence to:
Andre Stander

Email:
standerandre@gmail.com

Postal address:
Private Bag X323, Arcadia 0007, South Africa

Dates:
Received: 18 Nov. 2010
Accepted: 05 May 2011
Published: 14 Sept. 2011

How to cite this article:
Stander BA, Marais S, Huyser C, Fourie Z, Leszczynski D, Joubert AM. Effects of non-thermal mobile phone radiation on breast adenocarcinoma cells. S Afr J Sci. 2011;107(9/10), Art. #525, 9 pages. doi:10.4102/sajs.v107i9/10.525

Mobile phone usage currently exceeds landline communication in Africa. The extent of this usage has raised concerns about the long-term health effects of the ongoing use of mobile phones. To assess the physiological effects of radiation from mobile phones *in vitro*, MCF-7 breast adenocarcinoma cells were exposed to 2W/kg non-thermal 900-MHz mobile phone radiation. The effects investigated were those on metabolic activity, cell morphology, cell cycle progression, phosphatidylserine (PS) externalisation and the generation of reactive oxygen species and nitrogen species. Statistically insignificant increases in mitochondrial dehydrogenase activity were observed in irradiated cells when compared to controls. Fluorescent detection of F-actin demonstrated an increase in F-actin stress fibre formation in irradiated MCF-7 cells. Cell cycle progression revealed no statistically significant variation. A small increase in early and late apoptotic events in irradiated MCF-7 cells was observed. No statistically significant changes were observed in reactive oxygen and reactive nitrogen species generation. In addition, quantitative and qualitative analyses of cell cycle activity and nuclear and cytosolic changes, respectively, revealed no significant changes. In conclusion, exposure to 1 h of 900-MHz irradiation induced an increase in PS externalisation and an increase in the formation of F-actin stress fibres in MCF-7 cells. Data obtained from this study, and their correlation with other studies, provides intriguing links between radio frequency radiation and cellular events and warrant further investigation.

Introduction

Mobile phones form an integral part of the daily life of billions of users worldwide and this number is ever-increasing.[1] Because mobile phone technology emits low-energy electromagnetic fields (EMF), concerns have been raised as to whether exposure to non-ionising electromagnetic radiation in this radio frequency range can modify biological material, leading to possible adverse health effects.[2,3] In spite of previous *in vitro* and *in vivo* studies on the influence of mobile phone radiation on cell proliferation, cell differentiation, apoptosis induction, phosphorylation and changes in global gene expression, several questions still remain because of study limitations and conflicting results.

Leszczynski et al.[4] studied the activation of heat shock protein (HSP) 27 after 1 h exposure of EA.hy926 human endothelial cells to 900 megahertz (MHz) non-thermal radiation.[4] They observed an increase in the phosphorylation levels of HSP27, mediated by the p38 mitogen activated protein kinase (MAPK) pathway, which was also found to be transiently activated in response to radio frequency (RF)-EMF exposure.[4] Data suggested that the p38MAPK/HSP27 stress response pathway was induced as a result of RF-EMF exposure at non-thermal power levels.[4] In another study, the influence of 1 h of 900-MHz 2.4-W/kg specific absorption rate (SAR) exposure was investigated on EA.hy926 cells.[5] Protein expression levels of vimentin, which plays a role in cytoskeleton rearrangement, were statistically significantly affected. A 1-h exposure of EA.hy926 and EA.hy926v1 to 900-MHz 2.8-W/kg SAR and the effects of 900 MHz and 1800 MHz at 0.77 W/kg SAR on various immortalised and primary cells lines also demonstrated that the response is cell line specific. Different cell lines show diverse sensitivity levels to low level stimulus.[6,7]

Merola et al.[8] investigated the influence of 900-MHz radiation at 1 W/kg SAR at a maximum exposure time of 72 h on cell proliferation, cell differentiation and apoptosis in a neuroblastoma cell line (LAN-5) and no significant changes were observed. No statistically significant variation was observed in gene expression profiles after exposure of U87MG glioblastoma cells and C3H 10T1/2 mouse cells to RF-EMF.[9,10] A 2-h exposure of leukocytes to 900 MHz between 0.3 W/kg and 1.0 W/kg SAR, as well as lymphocyte exposure to 935 MHz at either 1 W/kg or 2 W/kg SAR for 24 h, also revealed no genotoxic effects.[10,11,12] Yu et al.[13] reported no significant differences in the formation of mammary tumours and the proliferation thereof in female Sprague–Dawley rats. The rats were exposed to 900-MHz global system for mobile communications (GSM) radiation at SAR levels of 4.0 W/kg, 1.33 W/kg, 0.44 W/kg and 0 W/kg for 4 h per day, 5 days per week for a duration of 26 weeks.

Thus, because of the conflicting results reported and because epidemiological studies lack the necessary sensitivity to detect minor effects of mobile phone radiation, the need for a new approach in this field was proposed.[2,3,14] Because low-level EMF radiation may cause subtle physiological changes, the need for sensitive high-throughput screening techniques exists in order to more accurately measure the effects of EMF radiation on human tissue. *In vitro* data can rapidly increase the knowledge pool regarding the influence of mobile phone use on human health and supplement epidemiological studies. The aim of this *in vitro* study was to determine the influence of non-thermal 900-MHz mobile phone radiation on metabolic activity, cell morphology, cell cycle progression, phosphatidylserine (PS) externalisation and reactive oxygen species and nitrogen species generation in the MCF-7 breast adenocarcinoma cell line.[15]

Materials and methods

Heat-inactivated foetal calf serum (FCS), Dulbecco's minimum essential medium Eagle (D-MEM), penicillin, streptomycin and fungizone were purchased from Highveld Biological (Pty) Ltd. (Johannesburg, South Africa). Sterile cell culture flasks and plates were obtained through Lasec SA (Pty) Ltd. (Johannesburg, South Africa). Glass Petri dishes (with diameters of 55 mm) were supplied by Merck Chemicals (Pty) Ltd (Johannesburg, South Africa). An Annexin V-FITC kit from Miltenyi Biotec (GmbH, Bergisch Gladbach, Germany) was purchased from BIOCOM Biotech (Pty) Ltd (Pretoria, South Africa). An Alexa Fluor™ 488 phalloidin antibody was procured from The Scientific Group (Johannesburg, South Africa). A fluorescence-activated cell sorting FC500 system flow cytometer equipped with an air-cooled argon laser excited at 488 nm was acquired from Beckman Coulter South Africa (Pty) Ltd (Pretoria, South Africa). All other chemicals were of analytical grade and were obtained from Sigma Chemical Co. (St. Louis, MO, USA).

Cell culture

The MCF-7 cell line (human breast epithelial adenocarcinoma) was supplied by Highveld Biological (Pty) Ltd (Johannesburg, South Africa). Cells were grown and maintained in 25-cm^2 tissue culture flasks in a humidified atmosphere at 37 °C and 5% CO_2 in a Forma Scientific water-jacketed incubator (Marietta, OH, USA). MCF-7 cells were cultured in D-MEM and supplemented with 10% heat-inactivated FCS (56 °C, 30 min), 100 U/mL penicillin G, 100 µg/mL streptomycin and fungizone (250 µg/L). Experiments were conducted in Duroplan 55-mm-diameter glass Petri dishes. Exponentially growing cells were seeded at 500 000 cells per Petri dish in 3 mL maintenance medium. After a 24-h incubation period at 37 °C to allow for cell adherence, the medium was replaced to remove debris.

Experimental set-up and dosimetry

The RF-EMF exposure system was calibrated by T. Tiovo from the Functional Proteomics Group, Radiation Biology Laboratory (STUK, Helsinki, Finland). Cells were irradiated by an exposure system previously described.[4,16,17,18] Briefly, the RF-EMF signal was generated with an EDSG-1240 signal generator and modulated with a pulse duration of 0.577 ms and repetition rate of 4.615 ms to match the GSM signal modulation scheme. The signal was amplified with a RF-EMF Power Labs R720F amplifier (Radiation Biology Laboratory, STUK Radiation and Safety Authority, Helsinki, Finland) and fed to the exposure waveguide via a monopole type feed post. Cells were exposed for 1 h to a 900-MHz GSM-like signal at an average SAR of 2.0 W/kg. The SAR distribution in cell culture was determined using SEMCAD 1.8 software with a graded simulation grid.[19] More than 70% of the cells were within ±3 dB of the average SAR. A total of 440 000 voxels was used to simulate the medium, with the largest grid size in the culture medium being 0.1 mm x 0.1 mm x 0.1 mm. Simulation results were verified with temperature rise-based SAR measurements using a calibrated Vitek-type temperature probe (BSD Medical, Salt Lake City, UT, USA). Temperature measurements were also recorded to ensure constant temperature levels during exposures. SAR level (2 W/kg) temperatures ranged from 36.8 °C to 37.2 °C. MCF-7 cells placed outside the RF-EMF exposure chamber acted as controls.

Determination of metabolic activity

Metabolic activity was spectrophotometrically determined using 3-(4,5-dimethylthiazol-2-yl)-2,5-diphenyltetrazolium bromide (MTT) to measure intracellular levels of reduced nicotinamide adenine dinucleotide (NADH).[20] After a 1-h exposure carried out in triplicate, 300 µL of MTT (5 mg/mL in Phospate Buffered Saline) was added to each Petri dish containing 3 mL medium. The Petri dishes were incubated for 4 h at 37 °C in a 5% CO_2 incubator. Medium was carefully removed without disturbing the cells. Dimethyl sulphoxide (3 mL) was added to each Petri dish by gently pipetting up and down. The solution (100 µL) was transferred to wells (three wells per sample to give three technical replicates) of a clean microtitre plate and the absorbance was determined at 570 nm (reference 630 nm) with an EL_x800 Universal Microplate Reader from Bio-Tek Instruments Inc. (Winooski, VT, USA). The percentage of inhibition of the reduction of MTT was calculated in relation to control cells in each experimental series (control cells were assumed to have 100% metabolic activity).

Cell morphology: Haematoxylin and eosin staining

MCF-7 cells were seeded in a Petri dish on heat-sterilised cover slips. After 24-h attachment, the medium was discarded and the cells were exposed for 1 h to a 900-MHz GSM-like signal at an average SAR of 2.0 W/kg, before the cells were stained by standard haematoxylin and eosin staining procedures.[21] The cover slips were transferred to staining dishes and fixed with Bouin's fixative for 30 min. The Bouin's fixative was discarded and the cover slips were left in 70% ethanol for 20 min before they were rinsed with tap water. Mayer's haemalum was added and left for 20 min and then discarded. The cover slips were rinsed with tap water for

2 min and then with 70% ethanol before being subjected to 1% eosin for 5 min. The eosin was discarded and the cover slips were consecutively rinsed twice for 5 min with 70% ethanol, 96% ethanol, 100% ethanol and xylol. The cover slips were mounted on microscope slides with resin and left to dry. Cells were viewed using an inverted Carl Zeiss Axiovert 200 MRc5 microscope (Carl Zeiss (Pty) Ltd, Johannesburg, South Africa) and morphology recorded.

Cell morphology: Nuclear fluorescent microscopy

A dual fluorescent dye staining method utilising Hoechst 33342 and propidium iodide fluorescent dyes was used to detect nuclear morphological changes. Hoechst 33342 is a fluorescent dye that penetrates intact cell membranes of viable cells and cells undergoing apoptosis and stains the nucleus. Propidium iodide is a fluorescent dye that is unable to penetrate an intact membrane and therefore stains the nucleus of cells that have lost their membrane's integrity as a result of oncotic or necrotic processes. Exponentially growing MCF-7 cells were seeded in Petri dishes onto heat-sterilised cover slips. Immediately after exposure, 0.5 mL of Hoechst 33342 solution (3.5 μg/mL in PBS) was added to the medium to provide a final concentration of 0.9 μM and incubated for 30 min at 37 °C in a CO_2 incubator. After 25 min, 0.5 mL of propidium iodide solution (40 μg/mL in PBS) was added to the medium to provide a final concentration of 12 μM. Within 5 min the cover slips were mounted on microscope slides with mounting fluid (90% glycerol, 4% N-propyl-gallate, 6% PBS). Cells were examined with a Zeiss inverted Axiovert CFL40 microscope and Zeiss Axiovert MRm monochrome camera under Zeiss filter 2 for Hoechst 33342-stained cells and Zeiss filter 15 for propidium iodide-stained cells (Carl Zeiss (Pty) Ltd, Johannesburg, South Africa). In order to prevent fluorescent dye quenching, all procedures were performed in a dark room.

Cell morphology: F-actin fluorescent microscopy

The effect of a 1-h exposure to 900-MHz GSM RF-EMF on the formation of stress fibres and F-actin polymerisation was determined using fluorescein isothiocyanate (FITC)-conjugated phalloidin. Cells were seeded on glass cover slips and fixed with 3.7% paraformaldehyde in PBS after exposure. After rinsing with PBS, cells were permeabilised with 0.1% Triton X-100, rinsed with PBS and incubated in 0.1% bovine serum albumin (BSA) reconstituted in PBS. The BSA solution was removed and the cells were stained with Alexa Fluor™ 488 phalloidin, rinsed with water and mounted on a cover slip with Sigma Mounting Medium containing sodium phosphate and citric acid in glycerol. Cells were viewed and counted with an inverted Carl Zeiss Axiovert 200 MRc5 microscope (Carl Zeiss (Pty) Ltd, Johannesburg, South Africa).

Cell cycle progression: Flow cytometry

Flow cytometric analysis utilising propidium iodide as a nuclear stain was employed to monitor cell cycle progression. Cells were trypsinised and resuspended in 1 mL growth medium immediately after the 1 h exposure. Cells (1 x 10^6/mL) were centrifuged for 5 min at 300 g. The supernatant was discarded and the cells were resuspended in 200 μL of ice-cold PBS containing 0.1% FCS. Ice-cold 70% ethanol (4 mL) was added in a dropwise manner on a vortex to avoid cell clumping. Cells were stored at 4 °C for 24 h and subsequently centrifuged at 300 g for 5 min. The supernatant was removed and the cells were resuspended in 1 mL of PBS containing 40 μg/mL propidium iodide and 100 μg/mL RNase A. The solution was incubated at 37 °C and 5% CO_2 for 45 min. Propidium iodide fluorescence (FL3) was measured and data from at least 10 000 cells were analysed using the CXP software (Beckman Coulter South Africa (Pty) Ltd.). Data from cell debris (particles smaller than apoptotic bodies) and clumps of two or more cells were removed from further analysis. Cell cycle distributions from histograms generated by the CXP software were calculated with Multicycle (Phoenix Flow Systems, San Diego, CA, USA). Results are expressed as a percentage of the cells in each phase.

Apoptosis detection analysis: Flow cytometry

Annexin V was employed to measure the translocation of the membrane phospholipid phosphatidylserine (PS), which is associated with apoptotic processes. Annexin V is a 35 kDa – 36 kDa, calcium-dependent, phospholipid binding protein with a high affinity for PS. Cells were trypsinised and 1 x 10^6 cells were double-stained with Annexin V-FITC and propidium iodide, according to the manufacturer's instructions immediately after the 1-h exposure. Propidium iodide fluorescence (FL3) and Annexin V fluorescence (FL1) were measured and data from at least 30 000 cells were analysed using CXP software.

Hydrogen peroxide, superoxide and nitric oxide measurement: Flow cytometry

Hydrogen peroxide (H_2O_2) generation was assessed using 2,7-dichlorofluorescein diacetate (DCFDA), a non-fluorescent probe, which, upon oxidation by reactive oxygen species and peroxides is converted to the highly fluorescent derivative 2,7-dichlorofluorescein (DCF).[22] Superoxide generation was assessed using hydroethidine (HE). HE is oxidised by superoxide and not by hydroxyl radicals, singlet O_2, H_2O_2 or nitrogen radicals, to a red fluorescing compound.[23] Relative nitric oxide (NO) was measured by using the non-fluorescent probe, 4,5-diaminofluorescein diacetate (DAF2-DA). DAF-2 (4,5-diaminofluorescein) does not react with stable oxidised forms of NO such as NO_2^-, NO_3^-, nor with other reactive oxygen species such as superoxide, H_2O_2, and $ONOO^-$.[24] DAF2-DA is cell permeable and is hydrolysed by cytosolic esterases to DAF-2. In the presence of NO, the fluorescent product triazole (DAF-2T) is formed and measured via flow cytometry. After 1 h exposure, cells were trypsinised, washed with PBS and 1 x 10^6 cells were resuspended in 1 mL PBS. To prevent unnecessary loss of converted fluorescent compounds through membrane leakage, reactive oxygen species probes were added after trypsinisation. Cells were incubated with 20 μM DCFDA for 25 min and with 10 μM HE for 15 min at 37 °C. Hydrogen peroxide (20 μM) was added 5 min prior to measurement as a positive control for DCF

formation. For DAF2-DA, 5 µM was added to the cells in PBS and incubated for 45 min at 37 °C. DCF (FL1) fluorescence, DAF-2T (FL1) and the HE fluorescent product fluorescence (FL2) were measured (as described above) and data from at least 10 000 cells were analysed using CXP software.

Statistical analysis

Data were obtained from three independent experiments for all quantitative studies, expressed as the mean ± s.d. and statistically analysed for significance using the analysis of variance single factor model followed by a two-tailed Student's *t*-test. Means are presented in bar charts, with error bars indicating standard deviations; $p < 0.05$ was regarded as statistically significant. Qualitative studies were performed in triplicate. Percentage differences were calculated as follows: Percentage difference = [(Control/Exposed) (Control + Exposed)/2] x 100.

Results

Determination of metabolic activity

MTT was used to determine the ability of MCF-7 cells to reduce MTT to purple formazan crystals as a measurement of metabolic activity after 1 h of exposure to 900-MHz GSM radiation. Results indicate that metabolic activity and the ability of NADH to reduce MTT to formazan crystals were not affected by 1 h of 900-MHz GSM irradiation (Figure 1).

Cell morphology: Haematoxylin and eosin

The qualitative effects of a 1-h exposure to 900-MHz GSM on cell morphology were investigated by staining the nucleus and cytoplasm of MCF-7 cells with haematoxylin and eosin. Qualitatively no differences could be observed between the control (Figure 2A) and exposed cells (Figure 2B).

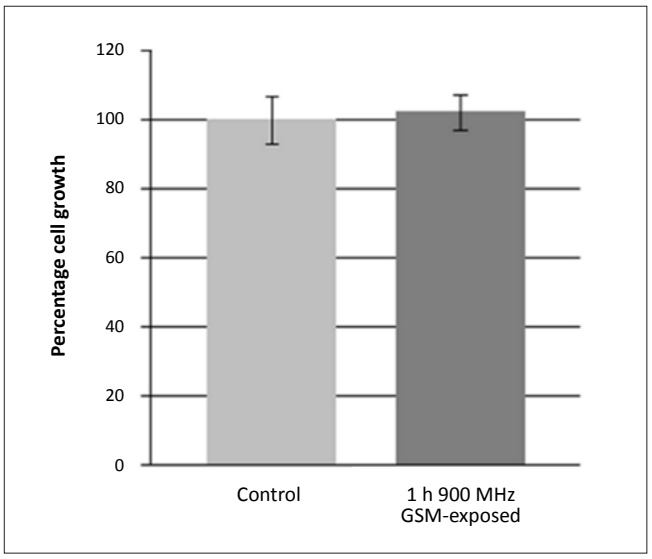

Values shown are the mean ± s.d. of three determinations.
No statistically significant difference in metabolic activity was observed ($p > 0.05$).

FIGURE 1: Metabolic activity of MCF-7 cells exposed to 900-MHz GSM for 1 h as a percentage of control cells (normalised to 1).

Cell morphology: Nuclear fluorescent microscopy

Qualitative analysis on nuclear morphology was conducted by staining the nucleus of control cells and cells exposed to 1 h of 900-MHz GSM radiation. No qualitative differences were observed and irradiated cells, when compared to the control cells (Figure 2C), exhibited normal nuclear morphology and cell division (Figure 2D).

Cell morphology: F-actin fluorescent microscopy

FITC-conjugated phalloidin was used to visualise F-actin filaments and fibres. As a positive control for thermal denaturation of F-actin, cells were exposed to 43 °C for 1 h. Aggregation of F-actin filaments and denaturation of F-actin fibres were observed in the thermally elevated (43 °C) positive control cells (Figure 3). The 900-MHz GSM-exposed cells did not exhibit any form of F-actin aggregation (Figure 4). However, actin stress fibre formation was observed and was more pronounced in irradiated cells when compared to control cells (Figures 4 and 5). A 'fuzzy-like' distribution of F-actin filaments was observed in the control cells; however, this was less pronounced in irradiated cells (Figures 4 and 5).

Cell cycle progression: Flow cytometry

DNA content analysis was conducted by means of flow cytometry (Figures 6A and 6B). Data analysis showed no statistically significant changes in cell cycle progression ($p > 0.1$) (Table 1).

Apoptosis detection analysis: Flow cytometry

Quantitative analyses of the externalisation of membrane phosphatidylserine with Annexin V were performed in order to detect early and late apoptotic processes (Figures 7A, 7B and 7C). Propidium iodide was used to measure the number of necrotic cells. Cells exposed to 900-MHz GSM radiation showed a statistically significant increase in PS externalisation relating to early and late apoptosis (percentage differences were 28.889% and 49.206%, respectively) (Table 2). Consequently, a small decrease in viable cells was also observed (percentage difference = –1.045%) (Table 2).

Hydrogen peroxide, superoxide and nitric oxide measurement: Flow cytometry

In order to investigate whether excess hydrogen peroxide and superoxide were produced in 900-MHz GSM-exposed cells compared to the control cells, flow cytometric analyses of MCF-7 cells loaded with the H_2O_2-sensitive fluorophore DCFDA, the superoxide sensitive probe HE and the NOS sensitive probe DAF2-DA were conducted. Figure 8A reveals a slight mean fluorescence decrease (0.87-fold; $p = 0.15$) in 900-MHz GSM-exposed cells (Figure 8B). HE mean fluorescence intensity was lower in 900-MHz GSM-exposed cells (0.95-fold that of control cells), but was also not considered statistically significant ($p = 0.09$) (Figures 9A and 9B). Average DAF-2T mean fluorescence intensity was lower in 900-MHz GSM-exposed cells (0.94-fold that of control cells), although also not statistically significantly so ($p = 0.21$) (Figures 10A and 10B).

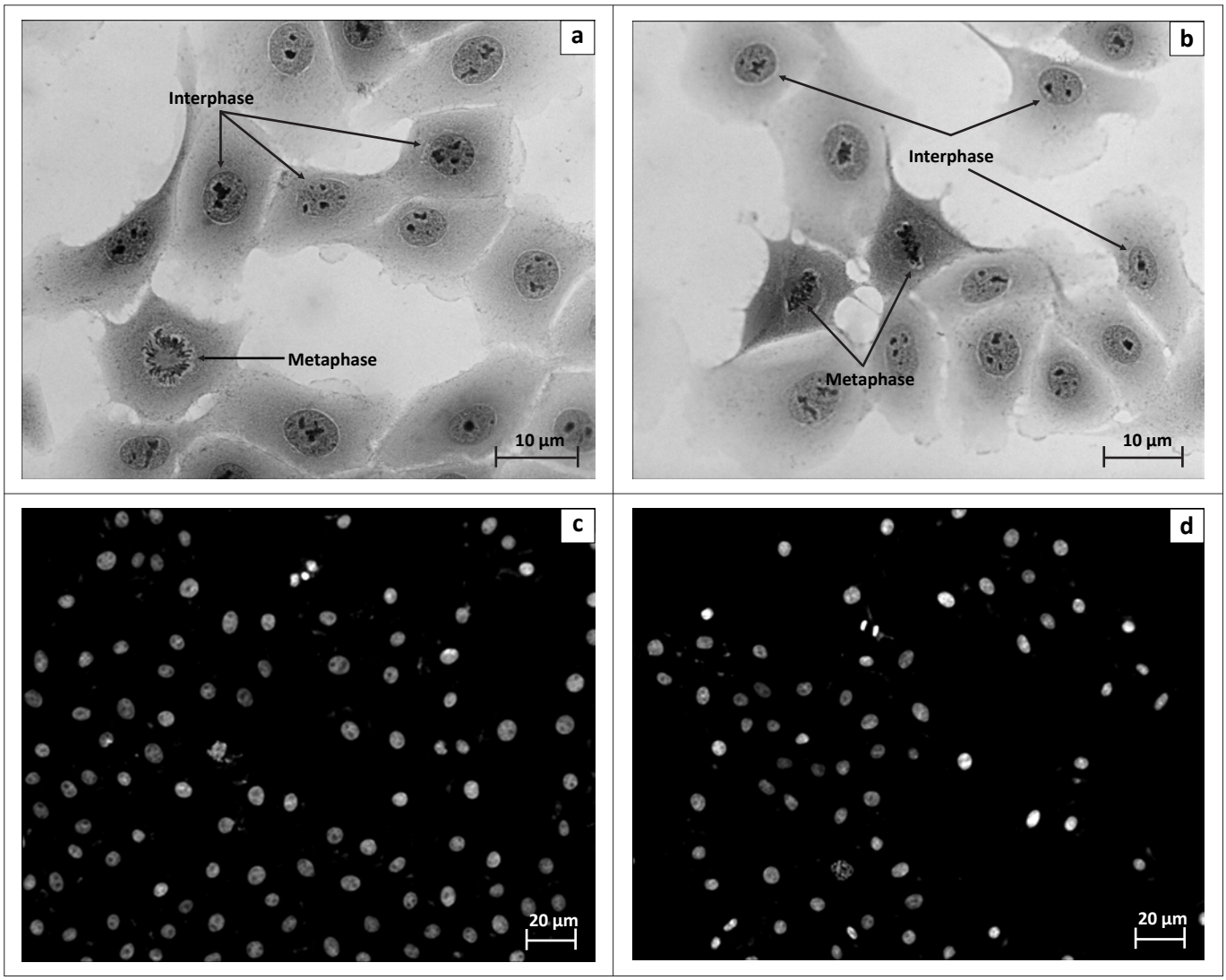

No qualitative differences were observed in nuclear and cytoplasmic morphology between control and exposed cells.

FIGURE 2: Haematoxylin and eosin (a and b) and Hoechst 33342 staining (c and d) of control (a and c) and 900-MHz GSM-exposed (b and d) MCF-7 cells.

Discussion

We investigated the effects of a 1-h exposure to 900-MHz GSM radiation on the metabolic activity, cell morphology, cell cycle progression, PS externalisation, and reactive oxygen species and nitrogen species generation of MCF-7 cells. Results revealed that metabolic activity and cell cycle activity were not affected and no nuclear and cytosolic changes were observed. Data are consistent with previous *in vitro* research conducted employing HEI-OC1 immortalised mouse auditory hair cells (exposed to 1763 MHz RF), Jurkat leukaemic T-cells (exposed to 1763 MHz RF) and U937 leukaemic monocyte lymphoma cells (exposed to 900 MHz RF) that also showed no difference in cell cycle distribution.[25,26,27]

However, conflicting data exist concerning the generation of reactive oxygen species in response to RF exposure in the literature. No changes in reactive oxygen species formation after 10 min and 30 min of exposure to 900 MHz RF were detected in L929 murine fibrosarcoma cells, whilst several studies on rats reported an increase in oxidative stress (an increase in malondialdehyde as an index of lipid peroxidation) and a decrease in superoxide dismutase, catalase and glutathione peroxidase activity.[28,29,30,31,32] Yurekli et al.[33] also reported an increase in oxidative stress and an increase in superoxide dismutase activity, whilst Balci et al.[34] reported an increase in oxidative stress and catalase activity in EMF-irradiated rat corneal tissue and no significant changes in rat lens tissue. Our results did not demonstrate any statistically significant differences, even though all the averages of the irradiated samples were less than the controls (H_2O_2 < 13%, superoxide < 5% and NOS < 4%).

An Annexin V-FITC assay was employed to measure the amount of PS residue translocated from the inner to the outer membrane as an indication of apoptosis. Differences in the externalisation of PS between control and exposed cells were observed. However, these changes revealed a less than 1% increase in early and late apoptosis and a small

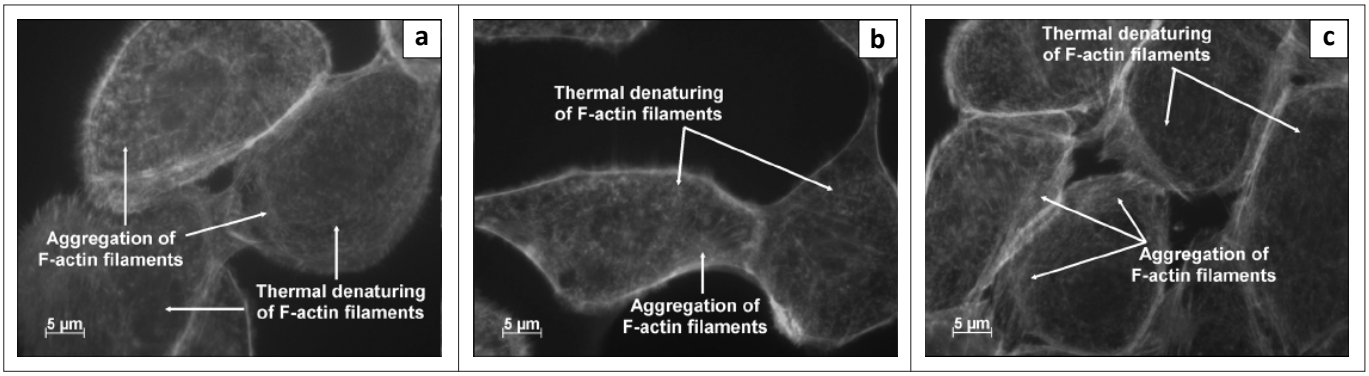

Aggregation of F-actin filaments as a result of thermal-induced denaturing was observed.

FIGURE 3: Fluorescein-isothiocyanate-conjugated phalloidin F-actin-stained MCF-7 cells (a–c) exposed to 43 °C for 1 h as a positive control for heat-induced F-actin morphological changes.

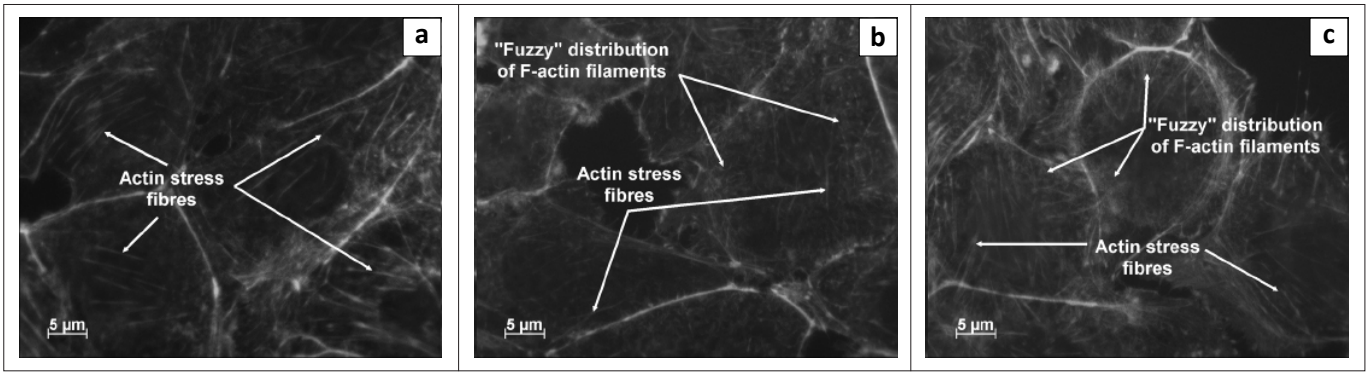

Actin stress fibre formations as well as a 'fuzzy-like' distribution of F-actin filaments were observed.

FIGURE 4: Fluorescein-isothiocyanate-conjugated phalloidin F-actin-stained MCF-7 cells (a–c) that were not exposed to 900-MHz GSM radiation.

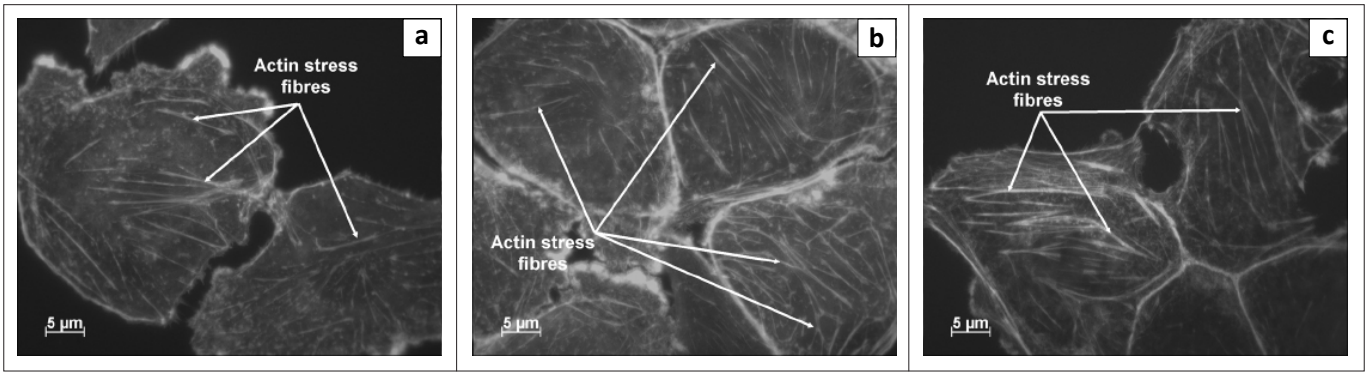

A more pronounced formation of actin stress fibres was observed when compared to the control. The 'fuzzy-like' distribution of F-actin filaments was also less pronounced when compared to the control.

FIGURE 5: Fluorescein-isothiocyanate-conjugated phalloidin F-actin-stained MCF-7 cells (a–c) after a 1-h exposure to 900-MHz GSM.

TABLE 1: Percentage change in MCF-7 cells in different phases of the cell cycle after a 1-h exposure to 900-MHz GSM radiation.

Phase of cell cycle	Control	Exposed	*p*-value	Difference (%)
Sub-G_1	1.63 ± 0.73	1.7 ± 0.59	0.960	0.025
G_1	51.54 ± 0.86	51.8 ± 1.01	0.726	0.262
S	36.04 ± 2.37	35.5 ± 1.27	0.746	–0.525
G_2/M	10.80 ± 1.90	11.0 ± 1.32	0.890	0.188

Sub-G_1, cells with DNA that is less than 2n and thus are dying; G_1, growth phase 1; S, synthesis phase; G_2, growth phase 2; M, mitosis.
Values shown are mean ± s.d. of three repeats.

TABLE 2: Measurement of phosphatidylserine externalisation and membrane permeability, as an indication of cells in various stages of cell death, of control and 900-MHz GSM-exposed MCF-7 cells after 1 h exposure.

Stages of cell death	Control	Exposed	*p*-value	Difference (%)
Early apoptosis	0.77 ± 0.10	1.03 ± 0.05	0.007	0.333
Late apoptosis	0.95 ± 0.26	1.57 ± 0.21	0.027	0.667
Necrosis	1.10 ± 0.34	1.23 ± 0.28	0.636	0.133
Viable cells	97.18 ± 0.40	96.17 ± 0.05	0.008	–1.133

Values shown are mean ± s.d. of three repeats.

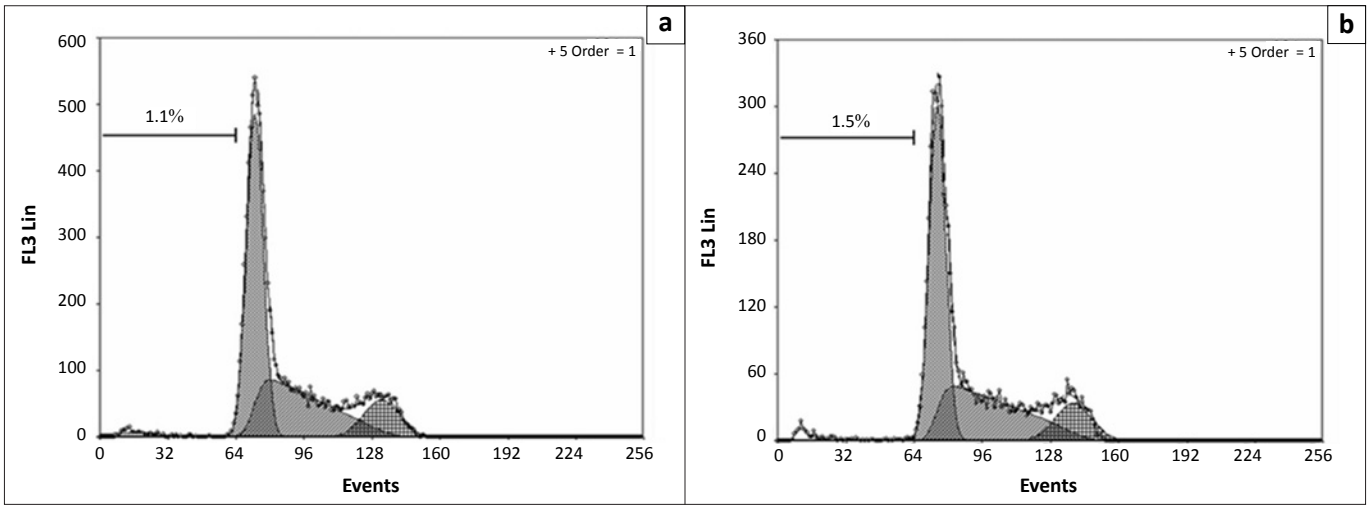

No statistically significant changes in cell cycle progression were observed.

FIGURE 6: Cell cycle histograms (FL3 Lin) of control (a) and 900-MHz GSM-exposed (b) MCF-7 cells.

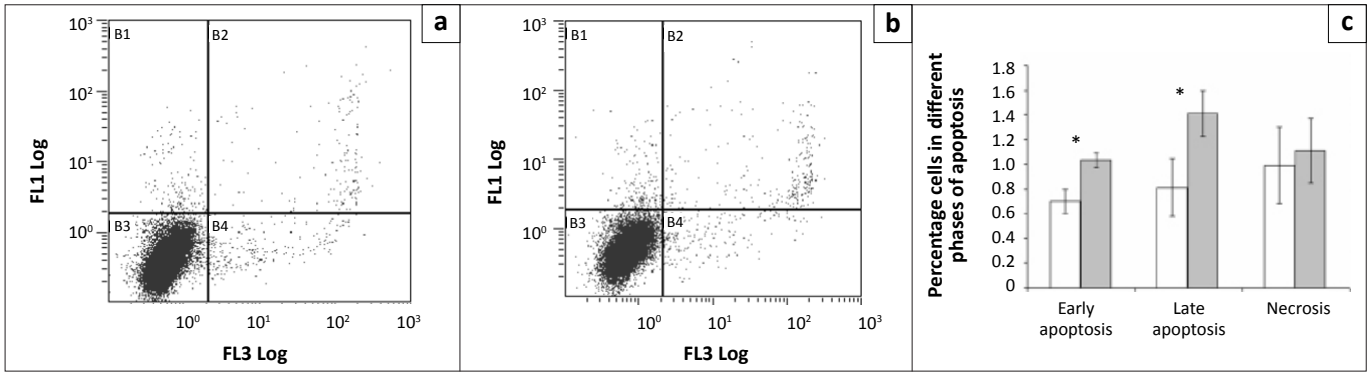

A statistically significant yet small increase in early (0.33%, $p = 0.007$) and late (0.67%, $p = 0.027$) apoptosis was observed in exposed MCF-7 cells, whilst a decrease in the number of viable cells (–1.13%, $p = 0.008$) was observed in exposed MCF-7 cells.
*$p < 0.05$

FIGURE 7: Propidium iodide (FL3 Log) versus Annexin V (FL1 Log) dot plot of control (a) and 900-MHz GSM-exposed (b) MCF-7 cells and (c) a comparison of the percentage of apoptotic cells in control (clear bars) and exposed (shaded bars) MCF-7 cells.

decrease (1.33%) in viable cells. No visible signs of increases in apoptosis were observed in morphological studies. It has been previously reported that cell death was not induced in monocytic U937, neuroblastoma SK-N-SH or neuroblastoma SH-SY5Y cells after exposure to 900-MHz RF.[27,35] An increase in caspase 3 activation in Jurkat T cells has been previously reported; however, this increase did not correspond to differences observed in the externalisation of PS.[36] Because MCF-7 cells do not express caspase 3,[37] the reason for the small increase in PS externalisation in response to a 1-h exposure to 900-MHz irradiation remains to be determined.

In this study, increased formation in F-actin stress fibres in irradiated cells was revealed when compared to the control. Our results are consistent with those of Nylund and Leszczynski[5]. These researchers reported a change from a 'fuzzy-like' to a 'fibrillar-like' staining of actin with phalloidin-stained EA.hy926 endothelial cells in response to 1 h of 900-MHz GSM RF radiation. Beta-actin exists as globular actin (G-actin) and filamentous actin (F-actin). G-actin polymerises into F-actin in response to extracellular signals.[38] G-actin also regulates NO synthesis activity through the regulation of nitric oxide synthase (NOS) at the post-transcriptional and post-translational levels.[39] In the same study by Su et al.[39], it was also observed that vimentin, a class III intermediate filament, was up-regulated. Remondini et al.[7] reported an up-regulation of caveolin 1, although it was not statistically significant. Interaction between caveolin 1 and NOS results in an inhibitory effect on NOS activity and NOS needs to be released from caveolin before it can be activated.[40] Nylund et al.[6] demonstrated that heat shock protein 90 (HSP90) was down-regulated in the EA.hy926 cell line. HSP90 is another NOS-interacting protein and needs to bind to actin to activate NOS. Activity of purified NOS-3 is higher when incubated with G-actin than when incubated with F-actin and NOS-3 does not co-localise with F-actin stress fibres.[39,41] Our findings that F-actin stress fibre formation was increased, can possibly be linked to NO signalling events linked with decreased HSP90 expression and increased caveolin 1 in response to RF radiation.

In conclusion, we found no statistically significant changes in mitochondrial dehydrogenase activity, or in reactive oxygen species and reactive nitrogen species generation. Also, quantitative analysis of cell cycle activity and qualitative analysis of nuclear and cytosolic changes revealed no significant effect. An increase in PS externalisation and an

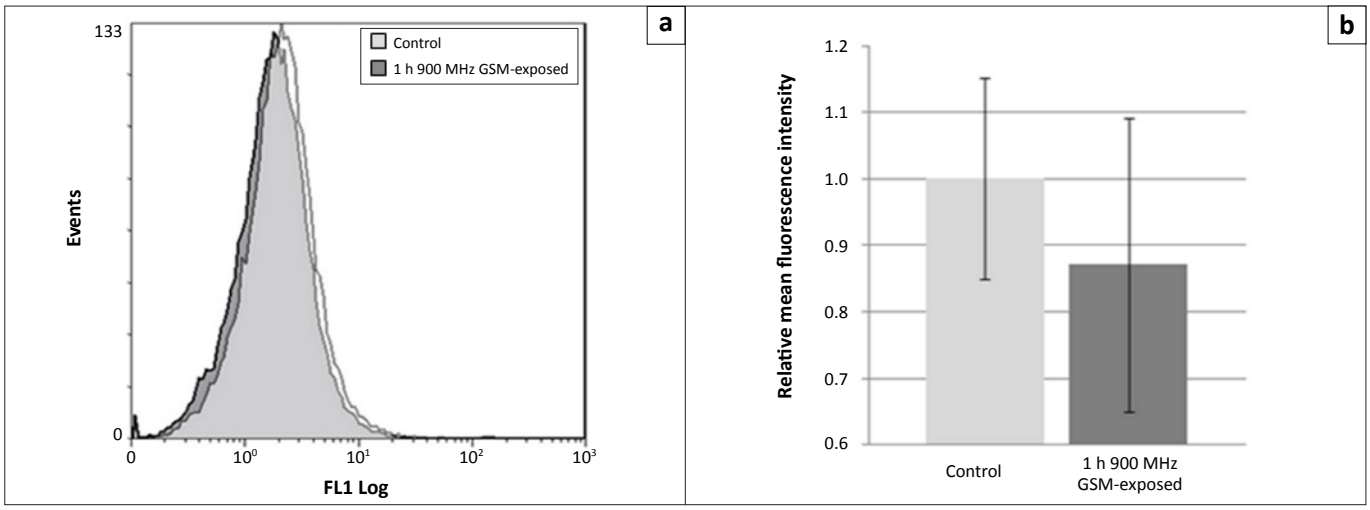

FIGURE 8: Relative mean fluorescence intensity of 2,7-dichlorofluorescein (FLG1 histogram) (a) in control (normalised to 1) and 900-MHz GSM-exposed MCF-7 cells after 1 h exposure. A non-significant decrease (0.87, $p = 0.15$) in relative mean fluorescence intensity of 2,7-dichlorofluorescein was observed in 900-MHz GSM-exposed cells (b).

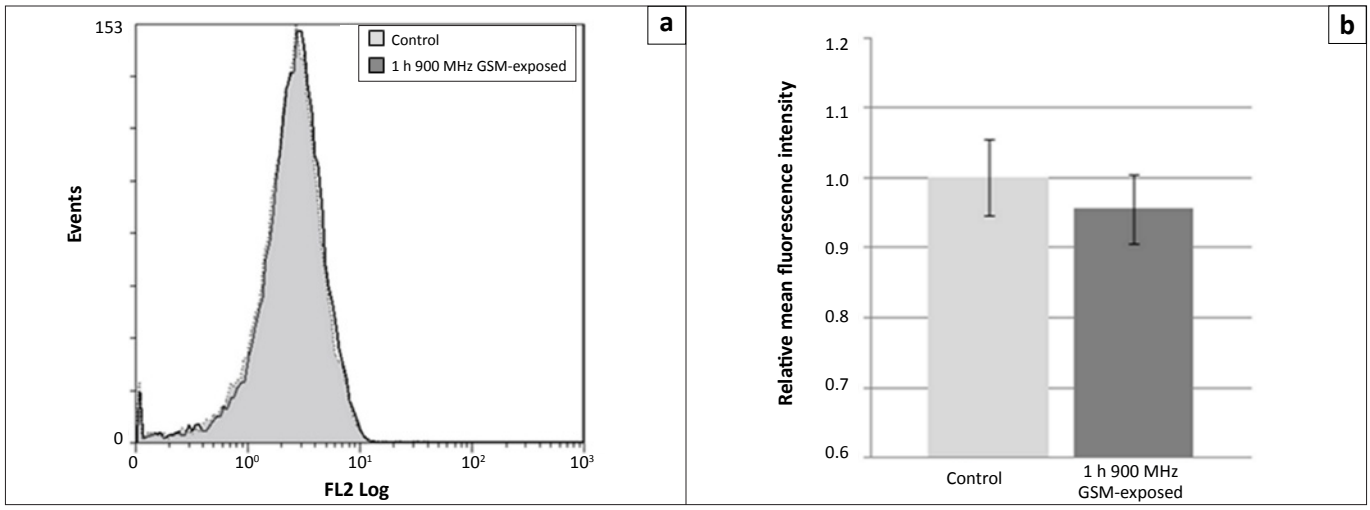

FIGURE 9: Relative mean fluorescence intensity of hydroethidine (FLG2 histogram) (a) in control (normalised to 1) and 900-MHz GSM-exposed MCF-7 cells after 1 h exposure. A non-significant decrease (0.95, $p = 0.09$) in relative mean fluorescence intensity of hydroethidine was observed in 900-MHz GSM-exposed cells (b).

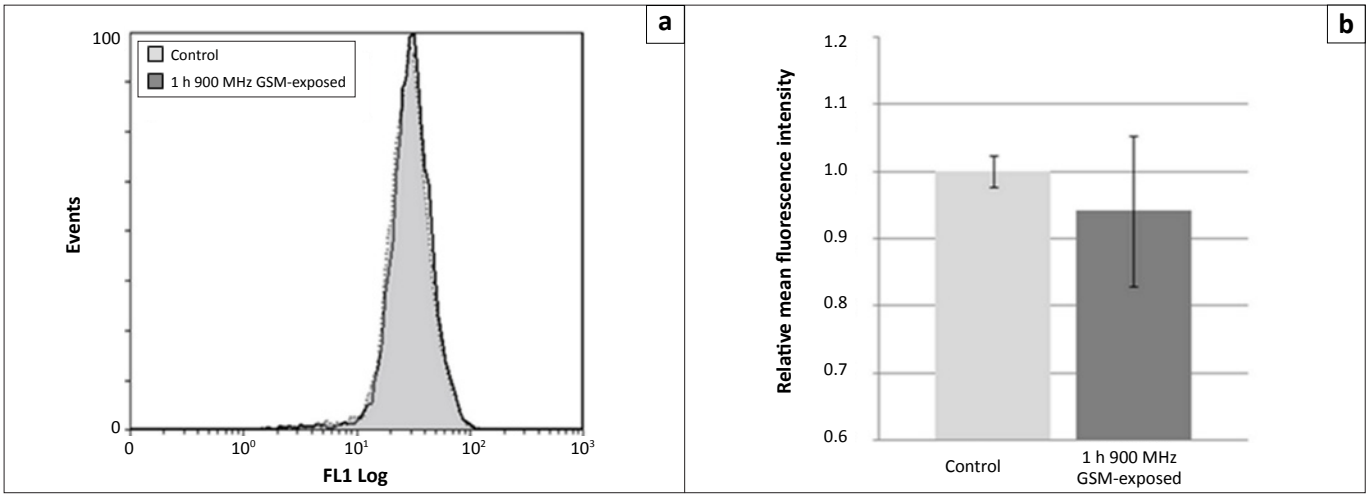

FIGURE 10: Relative mean fluorescence intensity of triazole (FLG1 histogram) (a) in control (normalised to 1) and 900-MHz GSM-exposed MCF-7 cells after 1 h exposure. A non-significant decrease (0.94, $p = 0.21$) in relative mean fluorescence intensity of triazole was observed in 900-MHz GSM-exposed cells (b).

increase in the formation of F-actin stress fibres observed in MCF-7 cells after a 1-h exposure to 900-MHz irradiation were demonstrated. Data obtained from this study and their correlation with other studies provide intriguing links between RF-radiation and cellular events and warrant further investigation.

Acknowledgements

This research was supported by grants from the Medical Research Council of South Africa (AG374, AK076), the Cancer Association of South Africa (AK246), the Struwig-Germeshuysen Cancer Research Trust of South Africa (AJ038, AN074) and the South African Bureau of Standards (AK386, AK387). Flow cytometric analyses were performed at the Department of Pharmacology at the Faculty of Health Sciences (University of Pretoria, Pretoria, South Africa). The authors would like to acknowledge Dr Nadia Falzone (Department of Biomedical Science, Faculty of Health Sciences, Tshwane University of Technology, Pretoria, South Africa) and Mr Tim Tiovo of the Functional Proteomics Group, Radiation Biology Laboratory, STUK Radiation and Safety Authority, Helsinki, Finland for maintenance and calibration of the RF-EMF exposure system.

References

1. Ahlbom AGL, Kheifets L, Savitz D, Swerdlow A. International Commission for Non-ionizing Radiation Protection Standing Committee on Epidemiology: Epidemiology of health effects of radiofrequency exposure. Environ Health Perspect. 2004;112:1741–1754. PMid:15579422, PMCid:1253668
2. Leszczynski D, Nylund R, Joenvaara S, Reivinen J. Applicability of discovery science approach to determine biological effects of mobile phone radiation. Proteomics. 2004;4(2):426–431. doi:10.1002/pmic.200300646, PMid:14760712
3. Leszczynski D, Meltz ML. Questions and answers concerning applicability of proteomics and transcriptomics in EMF research. Proteomics. 2006;6(17):4674–4677. doi:10.1002/pmic.200600414, PMid:16888768
4. Leszczynski D, Joenvaara S, Reivinen J, Kuokka R. Non-thermal activation of the hsp27/p38MAPK stress pathway by mobile phone radiation in human endothelial cells: Molecular mechanism for cancer- and blood-brain barrier-related effects. Differentiation. 2002;70(2-3):120–129. doi:10.1046/j.1432-0436.2002.700207.x, PMid:12076339
5. Nylund R, Leszczynski D. Proteomics analysis of human endothelial cell line EA.hy926 after exposure to GSM 900 radiation. Proteomics. 2004;4(5):1359–1365. doi:10.1002/pmic.200300773, PMid:15188403
6. Nylund R, Leszczynski D. Mobile phone radiation causes changes in gene and protein expression in human endothelial cell lines and the response seems to be genome- and proteome-dependent. Proteomics. 2006;6(17):4769–4780. doi:10.1002/pmic.200600076, PMid:16878295
7. Remondini D, Nylund R, Reivinen J, et al. Gene expression changes in human cells after exposure to mobile phone microwaves. Proteomics. 2006;6(17):4745–4754. doi:10.1002/pmic.200500896, PMid:16878293
8. Merola P, Marino C, Lovisolo GA, Pinto R, Laconi C, Negroni A. Proliferation and apoptosis in a neuroblastoma cell line exposed to 900 MHz modulated radiofrequency field. Bioelectromagnetics. 2006;27(3):164–171. doi:10.1002/bem.20201, PMid:16437547
9. Qutob SS, Chauhan V, Bellier PV, et al. Microarray gene expression profiling of a human glioblastoma cell line exposed in vitro to a 1.9 GHz pulse-modulated radiofrequency field. Radiat Res. 2006;165(6):636–644. doi:10.1667/RR3561.1, PMid:16802863
10. Whitehead TD, Moros EG, Brownstein BH, Roti Roti JL. Gene expression does not change significantly in C3H 10T(1/2) cells after exposure to 847.74 CDMA or 835.62 FDMA radiofrequency radiation. Radiat Res. 2006;165(6):626–635. doi:10.1667/RR3560.1, PMid:16802862
11. Zeni O, Romano M, Perrotta A, et al. Evaluation of genotoxic effects in human peripheral blood leukocytes following an acute in vitro exposure to 900 MHz radiofrequency fields. Bioelectromagnetics. 2005;26(4):258–265. doi:10.1002/bem.20078, PMid:15832336
12. Stronati L, Testa A, Moquet J, et al. 935 MHz cellular phone radiation. An in vitro study of genotoxicity in human lymphocytes. Int J Radiat Biol. 2006;82(5):339–346. doi:10.1080/09553000600739173, PMid:16782651
13. Yu D, Shen Y, Kuster N, Fu Y, Chiang H. Effects of 900 MHz GSM wireless communication signals on DMBA-induced mammary tumors in rats. Radiat Res. 2006;165(2):174–180. doi:10.1667/RR3497.1, PMid:16435916
14. Leszczynski D. The need for a new approach in studies of the biological effects of electromagnetic fields. Proteomics. 2006;6(17):4671–4673. doi:10.1002/pmic.200690099, PMid:16933341
15. Collection ATC. Product description: MCF-7 [homepage on the Internet]. c2009 [cited 2011 July 19]. Available from: https://www.atcc.org/ATCCAdvancedCatalogSearch/ProductDetails/tabid/452/Default.aspx?ATCCNum=HTB-22&Template=cellBiology
16. Falzone N, Huyser C, Fourie F, Toivo T, Leszczynski D, Franken D. In vitro effect of pulsed 900 MHz GSM radiation on mitochondrial membrane potential and motility of human spermatozoa. Bioelectromagnetics. 2008;29(4):268–276. doi:10.1002/bem.20390, PMid:18163440
17. Falzone N, Huyser C, Franken DR. Comparison between propidium iodide and 7-amino-actinomycin-D for viability assessment during flow cytometric analyses of the human sperm acrosome. Andrologia. 2010;42(1):20–26. doi:10.1111/j.1439-0272.2009.00949.x, PMid:20078512
18. Falzone N, Huyser C, Becker P, Leszczynski D, Franken DR. The effect of pulsed 900-MHZ GSM mobile phone radiation on the acrosome reaction, head morphometry and zona binding of human spermatozoa. Int J Androl. 2011;34(1):20–26. doi: 10.1111/j.1365-2605.2010.01054.x
19. SEMCAD X. Reference manual for the SEMCAD simulation platform for electromagnetic compatibility, antenna design and dosimetry. Zurich: SPEAG-Schmid & Partner Engineering AG. Available from: http://www.semcad.com
20. Liu Y, Peterson DA, Kimura H, Schubert D. Mechanism of cellular 3-(4,5-dimethylthiazol-2-yl)-2,5-diphenyltetrazolium bromide (MTT) reduction. J Neurochem. 1997;69(2):581–593. doi:10.1046/j.1471-4159.1997.69020581.x
21. Lillie RD. Histopathologic technic and practical histochemistry. New York: McGraw-Hill; 1965.
22. Rothe G, Valet G. Flow cytometric analysis of respiratory burst activity in phagocytes with hydroethidine and 2′,7′-dichlorofluorescin. J Leukoc Biol. 1990;47(5):440–448. PMid:2159514
23. Zhao HKS, Zhang H, Joseph J, Nithipatikom K, Vásquez-Vivar J, Kalyanaraman B. Superoxide reacts with hydroethidine but forms a fluorescent product that is distinctly different from ethidium: Potential implications in intracellular fluorescence detection of superoxide. Free Radical Biol Med. 2003;34(11):1359–1368. doi:10.1016/S0891-5849(03)00142-4
24. Kojima H, Nakatsubo N, Kikuchi K, et al. Detection and imaging of nitric oxide with novel fluorescent indicators: Diaminofluoresceins. Anal Chem. 1998;70(13):2446–2453. doi:10.1021/ac9801723, PMid:9666719
25. Huang TQ, Lee MS, Oh E, Zhang BT, Seo JS, Park WY. Molecular responses of Jurkat T-cells to 1763 MHz radiofrequency radiation. Int J Radiat Biol. 2008;84(9):734–741. doi:10.1080/09553000802317760, PMid:18821387
26. Huang TQ, Lee MS, Oh EH, et al. Characterization of biological effect of 1763 MHz radiofrequency exposure on auditory hair cells. Int J Radiat Biol. 2008;84(11):909–915. doi:10.1080/09553000802460123, PMid:19016139
27. Gurisik E, Warton K, Martin DK, Valenzuela SM. An in vitro study of the effects of exposure to a GSM signal in two human cell lines: Monocytic U937 and neuroblastoma SK-N-SH. Cell Biol Int. 2006;30(10):793–799. doi:10.1016/j.cellbi.2006.06.001, PMid:16877012
28. Elhag MA, Nabil GM, Attia AM. Effects of electromagnetic field produced by mobile phones on the oxidant and antioxidant status of rats. Pak J Biol Sci. 2007;10(23):4271–4274. doi:10.3923/pjbs.2007.4271.4274
29. Guney M, Ozguner F, Oral B, Karahan N, Mungan T. 900 MHz radiofrequency-induced histopathologic changes and oxidative stress in rat endometrium: Protection by vitamins E and C. Toxicol Ind Health. 2007;23(7):411–420. doi:10.1177/0748233707080906, PMid:18536493
30. Oral B, Guney M, Ozguner F, et al. Endometrial apoptosis induced by a 900-MHz mobile phone: Preventive effects of vitamins E and C. Adv Ther. 2006;23(6):957–973. doi:10.1007/BF02850217, PMid:17276964
31. Ozguner F, Altinbas A, Ozaydin M, et al. Mobile phone-induced myocardial oxidative stress: Protection by a novel antioxidant agent caffeic acid phenethyl ester. Toxicol Ind Health. 2005;21(9):223–230. doi:10.1191/0748233705th228oa, PMid:16342473
32. Sokolovic D, Djindjic B, Nikolic J, et al. Melatonin reduces oxidative stress induced by chronic exposure of microwave radiation from mobile phones in rat brain. J Radiat Res (Tokyo). 2008;49(6):579–586. doi:10.1269/jrr.07077, PMid:18827438
33. Yurekli AI, Ozkan M, Kalkan T, et al. GSM base station electromagnetic radiation and oxidative stress in rats. Electromagn Biol Med. 2006;25(3):177–188. doi:10.1080/15368370600875042, PMid:16954120
34. Balci M, Devrim E, Durak I. Effects of mobile phones on oxidant/antioxidant balance in cornea and lens of rats. Curr Eye Res. 2007;32(1):21–25. doi:10.1080/02713680601114948, PMid:17364731
35. Joubert V, Leveque P, Rametti A, Collin A, Bourthoumieu S, Yardin C. Microwave exposure of neuronal cells in vitro: Study of apoptosis. Int J Radiat Biol. 2006;82(4):267–275. doi:10.1080/09553000600649232, PMid:16690594
36. Palumbo R, Brescia F, Capasso D, et al. Exposure to 900 MHz radiofrequency radiation induces caspase 3 activation in proliferating human lymphocytes. Radiat Res. 2008;170(3):327–334. doi:10.1667/RR1098.1, PMid:18763855
37. Janicke RU. MCF-7 breast carcinoma cells do not express caspase-3. Breast Cancer Res Treat. 2009;117(1):219–221.
38. Disanza A, Steffen A, Hertzog M, Frittoli E, Rottner K, Scita G. Actin polymerization machinery: The finish line of signaling networks, the starting point of cellular movement. Cell Mol Life Sci. 2005;62(9):955–970. doi:10.1007/s00018-004-4472-6, PMid:15868099
39. Su Y, Kondrikov D, Block ER. Beta-actin: A regulator of NOS-3. Sci STKE. 2007;2007(404):pe52. doi:10.1126/stke.4042007pe52, PMid:17878410
40. Thomas CM, Smart EJ. Caveolae structure and function. J Cell Mol Med. 2008;12(3):796–809. doi:10.1111/j.1582-4934.2008.00295.x, PMid:18315571
41. Ji Y, Ferracci G, Warley A, et al. β-Actin regulates platelet nitric oxide synthase 3 activity through interaction with heat shock protein 90. Proc Natl Acad Sci USA. 2007;104(21):8839–8844. doi:10.1073/pnas.0611416104, PMid:17502619, PMCid:1885589